Fluctuation analysis of the atmospheric energy cycle

Richard Blender,[*] Denny Gohlke,[†] and Frank Lunkeit[‡]
Meteorological Institute, University of Hamburg, Hamburg 20146, Germany

(Received 7 March 2018; revised manuscript received 18 May 2018; published 3 August 2018)

The atmosphere gains available potential energy by solar radiation and dissipates kinetic energy mainly in the atmospheric boundary layer. We analyze the fluctuations of the global mean energy cycle defined by Lorenz in a simulation with a simplified hydrostatic model. The energy current densities are well approximated by the generalized Gumbel distribution and the Generalized Extreme Value (GEV) distribution. In an attempt to assess the fluctuation relation of Evans, Cohen, and Morriss we define entropy production by the injected power and use the GEV location parameter as a reference state. The fluctuation ratio reveals a linear behavior in a finite range.

DOI: 10.1103/PhysRevE.98.023101

I. INTRODUCTION

The global atmosphere is a physical system driven to a nonequilibrium state by radiative forcing and friction in the atmospheric boundary layer. A well-known diagnostic scheme for the energy flow is the Lorenz energy cycle (LEC) [1], which includes the zonal mean and the eddy parts of the available potential and the kinetic energies and determines the injected power, the dissipated energy, and internal conversions. The LEC constitutes a network of energy currents and can be considered as an atmospheric energy cascade. For the ocean an analogous cycle can be defined [2]. The means in the LEC constitute the climate from a dynamical point of view, and the fluctuations are related to climate variability. The properties of the climatological LEC require three-dimensional fields, which are known from reanalysis data sets like ERA and NCEP [3]. These data sets are obtained by data assimilation and global atmospheric models.

Our data are produced in a simulation with the atmospheric model PUMA (Portable University Model of the Atmosphere, University of Hamburg [4]), which is a dynamical core based on the hydrostatic primitive equations implemented in complex weather and climate models. PUMA is subject to linear surface friction and hyperdiffusion. Since this model does not intend to simulate climate, it neglects a radiation scheme and the hydrological cycle (hence it is denoted as "dry"). Further compartments like an ocean or a soil model are not considered as well. The model is driven by a temperature relaxation towards a steady state close to observations. The neglect of complex parametrizations is outweighed by transparent physical equations and a high numerical efficiency.

Few results for fluctuations in nonequilibrium systems are known. A remarkable finding was that the fluctuation of global observables can be approximated by the generalized Gumbel distribution [5,6], which depends on a parameter k denoting the order of the maximum. This parameter was identified as $k \approx \pi/2$, hence a noninteger between the first and the second maximum. A special form of the gamma distribution (the chi-square distribution) has been fitted to the kinetic energy and the dissipation rate in a spring-block model [7]. Since different types of complex systems show the generalized Gumbel distribution, a common origin can be assumed. Hypotheses for the occurrence of this distribution are self-similarity, extremal processes, and correlations [8,9]. Since the energy currents in the LEC are global averages and the turbulent atmosphere is highly correlated, it is worthwhile to test whether the fluctuations follow this distribution.

The Fluctuation Theorem (FT) [10–14] relates the probabilities of negative and positive entropy productions in nonequilibrium physical systems. This deviation from the second law is found on finite timescales for small (or mesoscopic) systems and vanishes in the thermodynamic limit. Gallavotti and Cohen provided a proof of the FT for time-reversible Anosov systems [11,12]. Dewar derived the FT based on a maximum entropy production principle [15].

This study is guided by the steady state FT (see, e.g., Refs. [12,13])

$$\lim_{\tau \to \infty} \frac{1}{\tau} \ln \frac{P(p_\tau = A)}{P(p_\tau = -A)} = \sigma_+ A \tag{1}$$

for the ratio $p_\tau = \sigma_\tau/\sigma_+$ of the time averages σ_τ of the entropy production σ in τ windows (beyond the relaxation to the steady state) and the long-term mean σ_+. The FT can be derived for the so-called dissipation function defined in phase space which needs identification with an entropy-like macroscopic observable [16]. In the following we will use the common notion fluctuation relation (FR) for (1).

The FT has been observed in a large number of laboratory and numerical experiments using different observables. In experiments the relation (1) is valid for timescales τ well above characteristic timescales. Rayleigh-Bénard convection was studied in Ref. [17] for the local entropy production as observable. In numerical experiments of thermal convection, the authors of Ref. [18] analyzed the work term along Lagrangian paths as a representation of the entropy production rate. The work by the turbulent pressure force in two experiments was subjected to an FT analysis in Ref. [19]. The relation (1) was

[*]richard.blender@uni-hamburg.de
[†]denny.gohlke@uni-hamburg.de
[‡]frank.lunkeit@uni-hamburg.de

found with modified slopes depending on the chosen time window, and the impact of a new reference state was briefly considered. The injected power was used as an observable in different physical systems including the GOY turbulence shell model [7]. A common problem in experimental data is the sparsity of negative data [7]. In experiments with the model PUMA finite time Lyapunov exponents for the global circulation were observed with a frequency compatible with the FT [20]. In all these hydrodynamic experiments the time reversibility as a condition for the validity of the FT is not satisfied. Ciliberto *et al.* [21] review applications of the FT to experimental data and consider in particular the appropriate choice of the entropy-like observable, time reversibility, and possible prefactors of $\sigma_+ A$ on the right-hand side of relation (1). In a step towards the analysis of the FT in a climatological context, Ref. [22] has found negative values of the coarse-grained entropy production in a linear stochastic model based on concepts of stochastic thermodynamics [23] for the observed tropical sea surface temperature (in the period 1950–2000).

Our aim is twofold: First, we determine the probability distributions of the energy input, the dissipated energy, and the internal currents (conversions). We compare the generalized Gumbel distribution and the Generalized Extreme Value (GEV) distribution. In the second step we attempt to assess the fluctuation relation. Thus, our approach is closely related to Ref. [24] on wave turbulence and to Ref. [25] on an electric circuit. In both studies the FT could not be verified. A major problem in our LEC data is the low frequency of negative data. Furthermore, a reference state like the mean temperature in Rayleigh-Bénard convection [17,19] is less clear in the global atmosphere. Motivated by Ref. [17] where the mode (peak) of the observed local convective heat flux distribution and Ref. [24] where the mode of the injected power is close to zero, we test the idea to shift the currents to reference states. The first is the location parameter of the fitted GEV distribution, which is close to the mode in our data, the second reference state is the mean, and the third is the mode of the distribution; mean and mode are independent of the fitted distribution. The observed mean temperature has been used in Ref. [18] as a reference state, and the shift to an arbitrary reference state has been briefly considered in Ref. [19]. In simulated data a method like the large deviation algorithm [26] might be useful to increase the frequency of rare events.

The paper is organized as follows: The model is described in Sec. II, and the Lorenz energy cycle is defined in Sec. III. The results for the densities are in Sec. IV and for the fluctuation ratios in Sec. V. A summary and discussion are included in Sec. VI.

II. GLOBAL CIRCULATION MODEL

To determine energy currents we use the model PUMA (Portable University Model of the Atmosphere, University of Hamburg) [4,27]), a hydrostatic global atmospheric model based on the primitive equations on the sphere. The model simulates the large-scale atmospheric dynamics [28] and does not make use of complex parametrizations (mostly representations of subscale processes which have to be added in weather and climate models). In PUMA only the forcing and the friction are parameterized in linear terms (for details see below). The model is driven towards an artificial zonal mean temperature [29], which is chosen such that the mean state (model climate) is close to the observations.

The dynamical variables are the relative vorticity (according to the meteorological usage the vertical component of the vortex vector), the horizontal divergence, temperature, and the logarithm of the surface pressure. The set of equations is the following:

$$\partial_t \xi = s^2 \partial_\lambda \mathcal{F}_v - \partial_\mu \mathcal{F}_u - \frac{1}{\tau_f}\zeta - K\nabla^8 \zeta, \tag{2}$$

$$\partial_t D = s^2 \partial_\lambda \mathcal{F}_u + \partial_\mu \mathcal{F}_v - \nabla^2\left[\frac{s^2}{2}(U^2+V^2) + \Phi + \bar{T}\ln p_s\right] - \frac{1}{\tau_f} D - K\nabla^8 D, \tag{3}$$

$$\partial_t T' = -s^2\partial_\lambda(UT') - \partial_\mu(VT') + DT' - \dot{\tilde{\sigma}}\frac{\partial T}{\partial\tilde{\sigma}} + \kappa\frac{T\omega}{p} + \frac{1}{\tau_c}(T_R - T) - K\nabla^8 T', \tag{4}$$

$$\partial_t \ln p_s = -s^2 U\partial_\lambda \ln p_s - V\partial_\mu \ln p_s - D - \frac{\partial\dot{\tilde{\sigma}}}{\partial\tilde{\sigma}}, \tag{5}$$

$$\frac{\partial\Phi}{\partial\ln\tilde{\sigma}} = -T, \tag{6}$$

with $\mu = \sin\phi$ and $s^2 = 1/(1-\mu^2)$. The variables ζ and ξ denote absolute and relative vorticity, $\zeta = \xi + f$, f is the Coriolis parameter, D is the horizontal divergence, and p_s is the surface pressure. The temperature T is divided into the background, $\bar{T}$, and the anomaly, T'. Spherical coordinates are λ and ϕ for longitude and latitude. Φ is the geopotential, κ the adiabatic coefficient, and ω the vertical velocity. We use the abbreviations $U = u\cos\phi$ and $V = v\cos\phi$ for the zonal and meridional velocities u, v, and the fluxes $\mathcal{F}_u = V\zeta - \dot{\tilde{\sigma}}\partial U/\partial\tilde{\sigma} - T'\partial\ln p_s/\partial\lambda$ and $\mathcal{F}_v = -U\zeta - \dot{\tilde{\sigma}}\partial V/\partial\tilde{\sigma} - T's^{-2}\partial\ln p_s/\partial\sin\phi$. The vertical coordinate is divided into equally spaced $\tilde{\sigma}$ levels, $\tilde{\sigma} = p/p_s$, with the pressure p and the surface pressure p_s. For more details refer to Refs. [4,27].

A stationary state is maintained by driving the model towards a constant temperature profile (Newtonian cooling) with a prescribed equator-to-pole gradient. This means that a term $(T_R - T)/\tau_c$ is added to the temperature equation, where τ_c is the heating-cooling timescale, T denotes the actual model temperature, and T_R refers to the prescribed reference temperature [29]. Dissipation is formulated as Rayleigh friction active in the boundary layer, i.e., terms $-\zeta/\tau_f$ and $-D/\tau_f$ are added to the equations for vorticity and divergence, where $\tau_f \approx 30$ days is the friction timescale. Hyperdiffusion ($\propto K\nabla^8$) with a coefficient K accounts for subscale processes and numerical stability.

The horizontal resolution is given by the total spherical wave number $\ell = 21$ with a triangle truncation and the vertical resolution is 10 vertical levels. The equations are numerically solved using the spectral transform method [30]: Linear terms are evaluated in the spectral domain while nonlinear products are calculated in grid point space. In this configuration the model has $O(10^5)$ degrees of freedom. The model is integrated

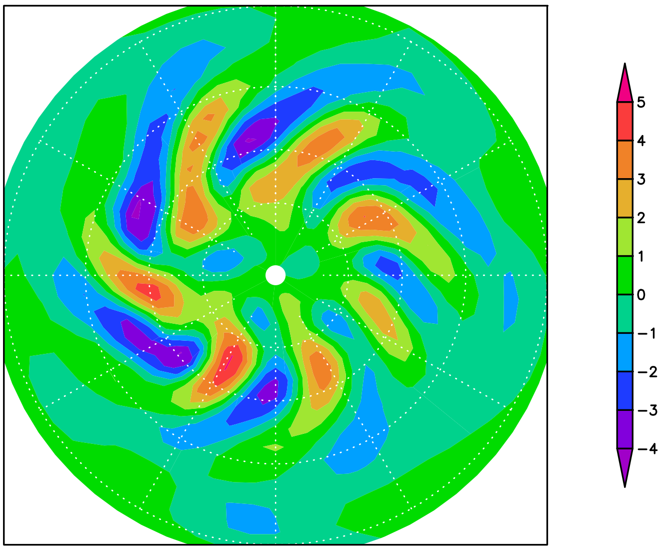

FIG. 1. Northern hemispheric relative vorticity in the midtroposphere (500 hPa) [10^{-5}/s].

by a leap-frog method with a time step of 15 min. Orography is not specified, and no external variability like annual or daily cycle is imposed ("equinox conditions"). The model supports baroclinic instability in the midlatitudes and the subsequent development of a turbulent state; see a snapshot of the relative vorticity ξ in Fig. 1.

III. LORENZ ENERGY CYCLE

The atmospheric Lorenz energy cycle (LEC) [1] describes the general circulation from a perspective that emphasizes energy transformations, i.e., how the incoming solar radiation generates potential energy that is transferred to kinetic energy and finally lost to frictional dissipation (Fig. 2). The LEC distinguishes the zonal mean and deviations thereof. These so-called eddies can be identified with synoptic cyclones and anticyclones, with a length-scale of thousand kilometers and a timescale of several days; they play an important role in the atmospheric energy cycle. An early assessment of the LEC can be found in Ref. [31]; for a recent analysis in reanalysis data NCEP2 and ERA40 see Ref. [3]. The characteristics of the global atmospheric energy cycle are useful for the validation of models, and it is expected that the Lorenz energy cycle changes in a warmer climate [32].

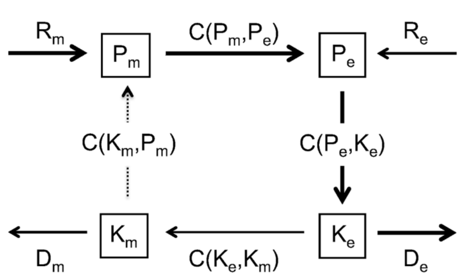

FIG. 2. Lorenz energy cycle with energy compartments (boxes) and energy currents (arrows). Available potential energy is P, kinetic energy is K, forcing is R, and dissipation is D; the zonal means are denoted by m and eddies by e. Internal conversions are $C(P_m, P_e)$, $C(P_e, K_e)$, $C(K_e, K_m)$, and $C(K_m, P_m)$. Intense currents are thick, moderate thin, and weak dotted.

We calculate the following terms in the energy cycle, and the expressions can be found in Ref. [1] or in Ref. [28]: the forcings of the zonal mean R_m and the eddy available potential energy R_e, the dissipation rates of zonal mean D_m, and the eddy kinetic energies D_e. Conversion rates are determined between the zonal means of the kinetic and the available potential energies $C(K_m, P_m)$, the zonal mean and eddy available potential energies $C(P_m, P_e)$, eddy available potential and kinetic energies $C(P_e, K_e)$, and eddy and zonal mean kinetic energies $C(K_e, K_m)$.

The model was run for 1000 years, and the LEC currents are determined as global means on a daily basis. For the interpretation it is relevant that the model is dry without convection and latent heat release. The forcing of the synoptic cyclones in nature deserves special attention since two processes contribute: (1) radiative forcing, which is zonally symmetric and attenuates deviations from the zonal mean, and (2) latent heat release, which forces the development of these eddies. In our dry model only a zonally symmetric part like (1) is included by the adjustment to a zonal mean temperature. This means that in our model the mean of R_e is negative.

If a hydrological cycle with latent heat release is included, this damping is compensated and the forcing R_e in observational data has a positive mean [3]. Note that forcing and dissipative terms are available only indirectly in the observational data.

IV. CURRENT DENSITIES

The frequency distributions of the forcing terms and the dissipative terms in the LEC are shown in Fig. 3. For the eddy forcing the negative values are included, $-R_e$, since the zonal mean forcing damps the eddies. The dissipative terms are split in the zonal mean part D_m and the eddy part D_e. The means of the external currents are R_m: 2.79, R_e: −1.18, D_m: 0.48, D_e: 1.12, and the means of the internal currents (conversions) are $C(P_m, P_e)$: 2.97, $C(P_e, K_e)$: 1.79, $C(K_e, K_m)$: 0.66, and $C(K_m, P_m)$: 0.18 (all values W/m^2). Note that the sign of the weak conversion $C(K_m, P_m)$ is unclear in observations [3].

The distributions can be approximated by the generalized Gumbel (GG) and the Generalized Extreme Value (GEV) distribution. In fits to the fluctuations of global quantities in correlated systems the generalized Gumbel distribution has been used (see Ref. [9] and references therein). The density of the generalized Gumbel distribution is

$$G_a(x) = \frac{\theta_a a^a}{\Gamma(a)} \exp\{-[\theta_a(x+\nu_a) + e^{-\theta_a(x+\nu_a)}]\} \tag{7}$$

with

$$\theta_a^2 = \frac{d^2 \ln \Gamma}{da^2}, \quad \nu_a = \frac{1}{\theta_a}\left(\ln a - \frac{d \ln \Gamma}{da}\right). \tag{8}$$

The GEV probability density is

$$f(z) = (1/s)(1+\xi z)^{-1-1/\xi}, \quad z = (x-\mu)/s, \tag{9}$$

with the location parameter μ, the scale s, and the shape parameter ξ. For a vanishing shape parameter ξ the GEV

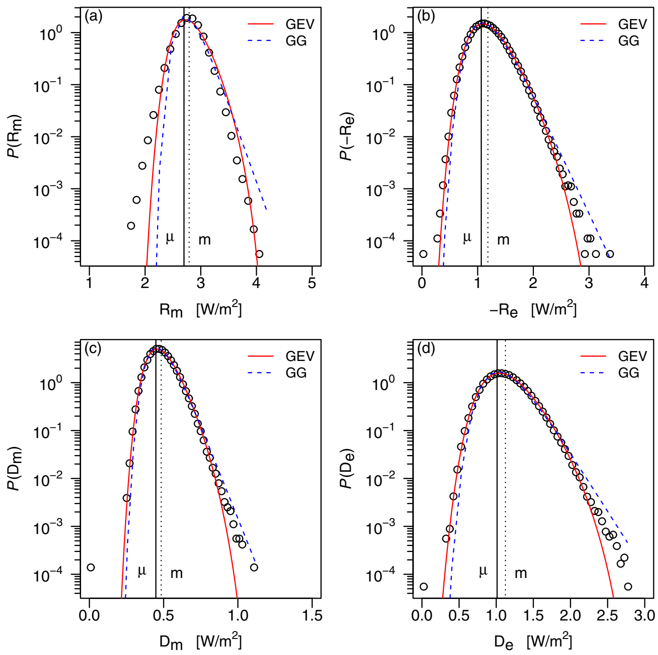

FIG. 3. Normalized histograms of energy input and dissipation: (a) zonal mean forcing (injected power) R_m, (b) negative eddy forcing $-R_e$, (c) zonal mean dissipation D_m, (d) eddy dissipation D_e. The solid (red) line is a GEV fit, and the dashed (blue) line a generalized Gumbel (GG) fit. The vertical lines indicate the GEV-location parameters μ (solid, black) and the means m (dotted, black).

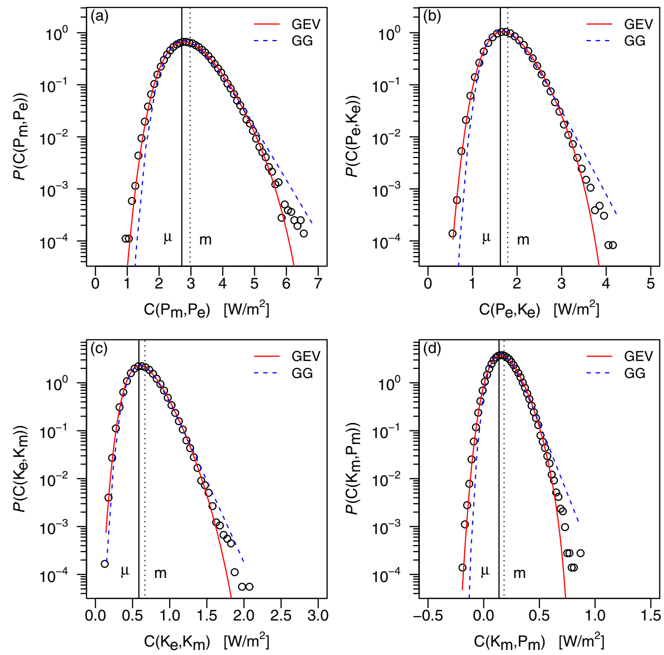

FIG. 4. Normalized histograms of internal currents (conversions): (a) zonal mean to eddy available potential energy $C(P_m, P_e)$, (b) eddy available potential energy to eddy kinetic energy $C(P_e, K_e)$, (c) eddy kinetic energy to zonal mean kinetic energy $C(K_e, K_m)$, (d) zonal mean kinetic energy to zonal mean potential energy $C(K_m, P_m)$. The fits are as in Fig. 3.

distribution reduces to the Gumbel distribution. The shape parameters ξ of the currents in the Figs. 3 and 4 are in the range $\xi \approx -0.2, \ldots, -0.1$. The skewness of the currents is positive and roughly 0.5.

As injected power in our model we consider the zonal mean forcing R_m of the available potential energy. The forcing of the eddies R_e is not considered since it damps eddies and has a negative mean (note that in nature solar radiation has a similar effect). Friction takes place mostly in the lowest levels which represent the atmospheric boundary layer, while the upper troposphere is only subject to hyperdiffusion.

The forcing of the zonal mean potential energy, which is the energy input in the present simulation, is used to define the entropy-like quantity in the nonequilibrium system,

$$\sigma = R_m, \tag{10}$$

with the long-term mean denoted by $\sigma_+ = \langle R_m \rangle$ (the eddy forcing R_e acts as a dissipation since the relaxation to a zonal mean temperature attenuates eddies). Note that the means satisfy

$$\langle R_m \rangle = \langle D_m + D_e - R_e \rangle. \tag{11}$$

Thus R_e should be added to $D_m + D_e$, and the common definition of an entropy production in terms of friction is not possible here.

V. FLUCTUATION RATIO

The ratio of negative to positive values in the currents is low and insufficient for an analysis of the fluctuation ratio (1). Therefore, we test shifts of the currents to reference states. In the following we consider three reference states J_R for the currents: (1) the location parameter μ of the fitted GEV distribution, (2) the mean of each current, and (3) the mode (pdf maximum) of each current.

The currents are transformed to anomalies

$$J' = J - J_R \tag{12}$$

with the reference state J_R.

The anomalies are averaged in windows with length τ:

$$J'_\tau = \frac{1}{\tau}\int_t^{t+\tau} J'(t')\,dt'. \tag{13}$$

All averaged current anomalies J'_τ are nondimensionalized by the long-term mean entropy production $\sigma_+ = \langle R_m \rangle$:

$$p_\tau = J'_\tau/\sigma_+. \tag{14}$$

The fluctuation ratio (1) is determined for the anomaly ratios p for the entropy production σ, and all other currents

$$\frac{1}{\tau}\ln\frac{P(p_\tau = A)}{P(p_\tau = -A)} = \alpha A \sigma_+, \tag{15}$$

where we have introduced a slope α. The normalized timescale $\tilde{\tau}$ is obtained by a typical correlation time of all currents, $\tau_c = 5$ days,

$$\tilde{\tau} = \tau/\tau_c. \tag{16}$$

In the original versions of the FT the factor α equals unity; this is not satisfied if the used entropy-like observable deviates from the entropy production as defined in Refs. [12,13].

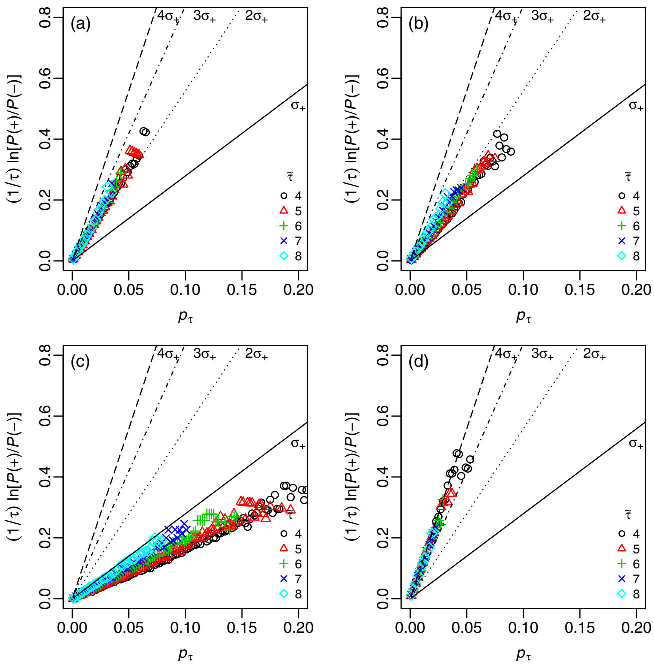

FIG. 5. Fluctuation ratio for the shift to the location parameters: (a) injected power $\sigma = R_m$ (defined as the entropy production), (b) eddy dissipation D_e, (c) conversion of zonally averaged potential to eddy potential energy $C(P_m, P_e)$, (d) i.i.d. GEV random variates r with the distribution of R_m.

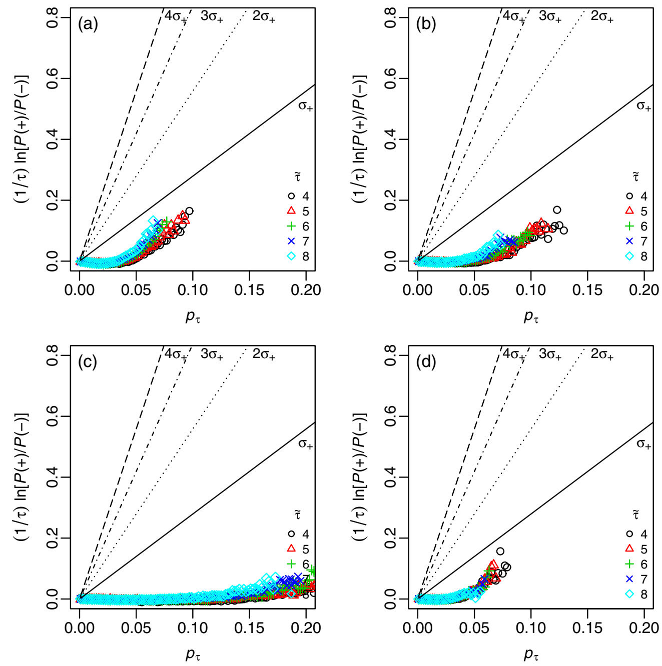

FIG. 6. Fluctuation ratio for the shift to the means of the current distributions: (a) injected power $\sigma = R_m$, (b) eddy dissipation D_e, (c) zonally averaged potential to zonally averaged kinetic energy conversion $C(P_m, P_e)$, (d) i.i.d. GEV random variates r with the distribution of R_m.

A. Location parameter as reference state

The first reference state J_R is the location parameter defined for each current by $J_R = \mu_J$, determined by a GEV fit to the current J. In Fig. 5 the results for (a) the injected power R_m, (b) the eddy dissipation D_e, (c) the current $C(P_m, P_e)$, and (d) surrogate data r are shown. The current $C(P_m, P_e)$ is used as an example to represent the currents in the LEC. The surrogate data r are independent random variables with a GEV distribution and parameters determined by a fit to R_m (injected power and entropy production σ). These data are added to extract the impact of the distribution independent of the correlations. Unfortunately, a robust quantitative estimation of the slopes is not possible (this is common in experimental data [21]), thus we refer to the slopes indicated in Fig. 5.

The fluctuation ratios in (15) for the injected power R_m are linear with slopes between $2\sigma_+$ and $3\sigma_+$. The eddy dissipation D_e reveals linear slopes of the order of $2\sigma_+$. The conversion $C(P_m, P_e)$ is linear with slopes below σ_+. The surrogate data r show slopes $\approx 4\sigma_+$ independent of the average time $\tilde{\tau}$ since the data are uncorrelated. The slope in the injected power does not reach this value even for the longest times analyzed. The deviation from $\alpha = 1$ is probably caused by an incorrect definition of the entropy production by the entropy-like quantity in (10).

B. Mean as reference state

For an assessment of the location parameter as the reference state we compare it to the mean of each current which could be considered as a first and nearby choice to increase the number of negative values. In Fig. 6 the results for the same currents as in Fig. 5 are shown. Obviously the fluctuation ratios are far from being linear. However, for large averaging times the slopes bend towards high values possibly close to the slopes obtained for the location parameter (Fig. 5).

C. Mode as reference state

As a further alternative for a reference state we have tested the mode M_J (the maximum of the pdf) for each current, $J_R = M_J$. The choice of the mode can be motivated by the observation of cusps in the distributions of fluxes in laboratory experiments, e.g., for the local convective heat flux in Rayleigh-Bénard convection [17] and the injected power in wave turbulence [24]. The results for the mode (not shown) are close to the results for the location parameter in Fig. 5. The reason is that the mode M of the GEV distribution is

$$M = \mu + s[(1+\xi)^{-\xi} - 1]/\xi, \tag{17}$$

which is close to the location parameter μ in our data, since $M \approx \mu - s\xi$, for small shape parameters as found here ($\xi = -0.2, \ldots, -0.1$). A clear advantage of the mode is that it can be estimated without an assumption on the distribution.

VI. SUMMARY AND DISCUSSION

We have analyzed the atmospheric energy cycle defined by Lorenz [1] in a 1000-year simulation with a simplified atmospheric model. The Lorenz energy cycle (LEC) assesses the energy cascade in the atmosphere by a separation of the total energy in available potential and kinetic energy and a split in zonal parts and deviations (the so-called eddies). Energy is injected as the forcing of the available potential energy and removed by frictional dissipation of kinetic energy. Both apply to the zonal mean and the eddy parts. The assessment of the realistic LEC needs three-dimensional atmospheric data, which are available only as model output; most common are the reanalysis data sets ERA and NCEP compared in Ref. [3] for the period 1979–2001.

Since an analysis of the FR is impossible with the short data sets available in complex climate models (order of 100 years; see, e.g., Ref. [32]), the LEC data used here with the duration of 1000 years are produced with the simplified atmospheric model PUMA [4]. PUMA simulates the so-called dynamical core based on the hydrostatic primitive equations. The simplification is obtained by the neglect of a radiation scheme and the hydrological cycle. Thus the model represents the nonlinear physical dynamics without complex processes like, for example, cloud formation and precipitation. The forcing is given by a linear temperature adjustment and friction by a drag of the velocity, mainly at the lowest level. The forcing is chosen to obtain a steady state close to the observations.

The first finding is that the LEC current distributions can be approximated by the generalized Gumbel distribution [5,6] and the Generalized Extreme Value (GEV) distribution.

The second result pertains to the asymmetry of the distribution. After a shift to the GEV location parameter (as a new reference state) an asymmetry similar to the fluctuation ratio (FR) emerges for the considered energy currents. The entropy production σ in this analysis is defined as the injected power. We define anomalies of the currents with respect to the reference states and nondimensionalize them with the long-term mean σ_+ of the entropy production. A nondimensional timescale is defined by $\tilde{\tau} = \tau/\tau_c$, where $\tau_c = 5$ days is a typical correlation timescale of the currents.

The shift to a reference state is motivated by the analysis of observational [17] and simulated data [24] where the maximum of the pdf (mode) is close to zero. Further reference states considered here are the mean of the data and the mode of the distribution.

We find that for the location parameter reference state, the entropy production, the current $C(P_m, P_e)$ (zonal mean to eddy available potential energy conversion), and the eddy dissipation follow fluctuation relations with linear slopes in the range $\sigma_+ \ldots 4\sigma_+$. A surrogate data test is included which uses i.i.d. random variables distributed like the entropy production (available potential energy forcing). The slope for these data is close to $4\sigma_+$.

We would like to add a remark on time reversibility in our data. In meteorology a common notion is the so-called *free atmosphere* above the boundary layer (the lowest hundreds of meters where friction takes place) [28]. If we neglect friction on short timescales in the equations of motion (see Sec. II) and identify these as microscopic dynamics, it is reasonable to assume that the atmosphere is approximately time-reversible on the corresponding timescales. Therefore, it is possible that the FT applies to the components of the LEC.

Since no physical constraints for the distributions of atmospheric energy currents are known, we expect that our findings might be useful for model assessment, global warming studies [32], and possibly the behavior of extremes [33,34].

ACKNOWLEDGMENTS

We acknowledge the support by the German Research Foundation (DFG) CRC/Transregio project TRR 181-M4 ("Energy Transfers in Atmosphere and Ocean") and discussions with Dr. Christian Franzke and Prof. Valerio Lucarini. We thank the two anonymous reviewers who helped to improve the paper considerably.

[1] E. N. Lorenz, Available potential energy and the maintenance of the general circulation, Tellus **7**, 157 (1955).

[2] J.-S. von Storch, C. Eden, I. Fast, H. Haak, D. Hernández-Deckers, E. Maier-Reimer, J. Marotzke, and D. Stammer, An estimate of the Lorenz energy cycle for the world ocean based on the STORM/NCEP simulation, J. Phys. Oceanogr. **42**, 2185 (2012).

[3] L. Li, A. P. Ingersoll, X. Jiang, D. Feldman, and Y. L. Yung, Lorenz energy cycle of the global atmosphere based on reanalysis datasets, Geophys. Res. Lett. **34**, L16813 (2007).

[4] K. Fraedrich, E. Kirk, U. Luksch, and F. Lunkeit, The portable university model of the atmosphere (PUMA): Storm track dynamics and frequency variability, Meteorol. Zs. **14**, 735 (2005).

[5] S. T. Bramwell, P. C. W. Holdsworth, and J.-F. Pinton, Universality of rare fluctuations in turbulence and critical phenomena, Nature (London) **396**, 552 (1998).

[6] S. T. Bramwell, K. Christensen, J.-Y. Fortin, P. C. W. Holdsworth, H. J. Jensen, S. Lise, J. M. López, M. Nicodemi, J.-F. Pinton, and M. Sellitto, Universal Fluctuations in Correlated Systems, Phys. Rev. Lett. **84**, 3744 (2000).

[7] S. Aumaître, S. Fauve, S. McNamara, and P. Poggi, Power injected in dissipative systems and the fluctuation theorem, Eur. Phys. J. B **19**, 449 (2001).

[8] K. Dahlstedt and H. J. Jensen, Universal fluctuations and extreme-value statistics, J. Phys. A **34**, 11193 (2001).

[9] E. Bertin, Global Fluctuations and Gumbel Statistics, Phys. Rev. Lett. **95**, 170601 (2005).

[10] D. J. Evans, E. D. G. Cohen, and G. P. Morriss, Probability of Second Law Violations in Shearing Steady States, Phys. Rev. Lett. **71**, 2401 (1993).

[11] G. Gallavotti and E. G. D. Cohen, Dynamical Ensembles in Nonequilibrium Statistical Mechanics, Phys. Rev. Lett. **74**, 2694 (1995).

[12] G. Gallavotti and E. G. D. Cohen, Dynamical ensembles in stationary states, J. Stat. Phys. **80**, 931 (1995).

[13] D. J. Evans and D. J. Searles, The fluctuation theorem, Adv. Phys. **51**, 1529 (2002).

[14] E. M. Sevick, R. Prabhakar, S. R. Williams, and D. J. Searles, Fluctuation theorems, Annu. Rev. Phys. Chem. **59**, 603 (2008).

[15] R. C. Dewar, Information theory explanation of the fluctuation theorem, maximum entropy production and self-organized criticality in non-equilibrium stationary states, J. Phys. A: Math. Gen. **36**, 631 (2003).

[16] O. G. Jepps and L. Rondoni, A dynamical-systems interpretation of the dissipation function, T-mixing and their relation to thermodynamic relaxation, J. Phys. A: Math. Theor. **49**, 154002 (2016).

[17] X.-D. Shang, P. Tong, and K.-Q. Xia, Test of steady-state fluctuation theorem in turbulent Rayleigh-Bénard convection, Phys. Rev. E **72**, 015301 (2005).

[18] F. Zonta and S. Chibbaro, Entropy production and fluctuation relation in turbulent thermal convection, Europhys. Lett. **114**, 50011 (2016).

[19] S. Ciliberto, N. Garnier, S. Hernandez, C. Lacpatia, J.-F. Pinton, and G. R. Chavarria, Experimental test of the Gallavotti-Cohen fluctuation theorem in turbulent flows, Physica A **340**, 240 (2004).

[20] B. Schalge, R. Blender, J. Wouters, K. Fraedrich, and F. Lunkeit, Evidence for a fluctuation theorem in an atmospheric circulation model, Phys. Rev. E **87**, 052113 (2013).

[21] S. Ciliberto, S. Joubaud, and A. Petrosyan, Fluctuations in out-of-equilibrium systems: From theory to experiment, J. Stat. Mech.: Theory Exp. (2010) P12003.

[22] J. B. Weiss, Nonequilibrium statistical mechanics of tropical sea surface temperature variability, Geophys. Res. Lett. **36**, L10705 (2009).

[23] U. Seifert, Entropy Production Along a Stochastic Trajectory and an Integral Fluctuation Theorem, Phys. Rev. Lett. **95**, 040602 (2005).

[24] É. Falcon, S. Aumaître, C. Falcón, C. Laroche, and S. Fauve, Fluctuations of Energy Flux in Wave Turbulence, Phys. Rev. Lett. **100**, 064503 (2008).

[25] C. Falcón and É. Falcon, Fluctuations of energy flux in a simple dissipative out-of-equilibrium system, Phys. Rev. E **79**, 041110 (2009).

[26] F. Ragone, J. Wouters, and F. Bouchet, Computation of extreme heat waves in climate models using a large deviation algorithm, Proc. Natl. Acad. Sci. USA **115**, 24 (2018).

[27] K. Fraedrich, A suite of user-friendly global climate models: Hysteresis experiments, Eur. Phys. J. Plus **127**, 53 (2012).

[28] J. R. Holton and G. J. Hakim, *An Introduction to Dynamic Meteorology*, Vol. 88, 5th Edition, International Geophysics Series (Academic Press, San Diego, 2012).

[29] I. M. Held and M. J. Suarez, A proposal for the intercomparison of the dynamical cores of atmospheric general circulation models, Bull. Am. Meteorol. Soc. **75**, 1825 (1994).

[30] S. A. Orszag, Transform method for calculation of vector coupled sums: Application to the spectral form of the vorticity equation, J. Atmos. Sci. **27**, 890 (1970).

[31] J. P. Peixóto and A. H. Oort, The annual distribution of atmospheric energy on a planetary scale, J. Geophys. Res. **79**, 2149 (1974).

[32] D. Hernandez-Deckers and J.-S. von Storch, Energetics responses to increases in greenhouse gas concentration, J. Clim. **23**, 3874 (2010).

[33] N. Merhav and Y. Kafri, Statistical properties of entropy production derived from fluctuation theorems, J. Stat. Mech.: Theory Exp. (2010) P12022.

[34] J. Gundermann, S. Siegert, and H. Kantz, Improved predictions of rare events using the Crooks fluctuation theorem, Phys. Rev. E **89**, 032112 (2014).